Hydroxylation and dechlorination of 3,3′,4,4′-tetrachlorobiphenyl (CB77) by rat and human CYP1A1s and critical roles of amino acids composing their substrate-binding cavity

Yabu, Miku ; Haga, Yuki ; Itoh, Toshimasa ; Goto, Erika ; Suzuki, Motoharu ; Yamazaki, Kiyoshi ; Mise, Shintaro ; Yamamoto, Keiko ;…

(Citation)
Science of the Total Environment,837:155848

(Issue Date)
2022-09-01

(Resource Type)
journal article

(Version)
Accepted Manuscript

(URL)
https://hdl.handle.net/20.500.14094/90009329

Hydroxylation and dechlorination of 3,3',4,4'-tetrachlorobiphenyl (CB77) by rat and human CYP1A1s and critical roles of amino acids composing their substrate-binding cavity

Miku Yabu[a], Yuki Haga[b], Toshimasa Itoh[c], Erika Goto[a], Motoharu Suzuki[b], Kiyoshi Yamazaki[a], Shintaro Mise[a], Keiko Yamamoto[c], Chisato Matsumura[b], Takeshi Nakano[d], Toshiyuki Sakaki[e], and Hideyuki Inui[a,f,]*

[a] Graduate School of Agricultural Science, Kobe University, 1-1 Rokkodaicho, Nada-ku, Kobe, Hyogo 657-8501, Japan

[b] Hyogo Prefectural Institute of Environmental Sciences, 3-1-18 Yukihiracho, Suma-ku, Kobe, Hyogo 654-0037, Japan

[c] Laboratory of Drug Design and Medicinal Chemistry, Showa Pharmaceutical University, 3-3165 Higashi-Tamagawagakuen, Machida, Tokyo 194-8543, Japan

[d] Research Center for Environmental Preservation, Osaka University, 2-4 Yamadaoka, Suita, Osaka 565-0871, Japan

[e] Department of Pharmaceutical Engineering, Faculty of Engineering, Toyama Prefectural University, 5180 Kurokawa, Imizu, Toyama 939-0398

[f] Biosignal Research Center, Kobe University, 1-1 Rokkodaicho, Nada-ku, Kobe, Hyogo 657-8501, Japan

*Corresponding Author

Hideyuki Inui, Biosignal Research Center, Kobe University, 1-1 Rokkodaicho, Nada-ku, Kobe, Hyogo, 657-8501, Japan

E-mail: hinui@kobe-u.ac.jp, Telephone number: +81-78-803-5863

ABSTRACT

Cytochrome P450 (CYP) monooxygenases play critical roles in determining the toxicity of polychlorinated biphenyls (PCBs) in mammals. Hydroxylation of PCBs by these enzymes leads to increased water solubility, promoting the elimination of PCBs from the body. The CYP1 family is mainly responsible for metabolizing PCBs that exhibit a dioxin-like toxicity. Although the dioxin-like PCB 3,3′,4,4′-tetrachlorobiphenyl (CB77) is abundant in the environment and accumulates in organisms, information on CB77 metabolism by CYP1A1s is limited. In this study, recombinant rat CYP1A1 metabolized CB77 to 4′-hydroxy (OH)-3,3′,4,5′-tetrachlorobiphenyl (CB79) and 4′-OH-3,3′,4-trichlorobiphenyl (CB35), whereas human CYP1A1 produced only 4′-OH-CB79. Rat CYP1A1 exhibited much higher metabolizing activity than human CYP1A1 because CB77 was stably accommodated in the substrate-binding cavity of rat CYP1A1 and was close to its heme. In a rat CYP1A1 mutant with two human-type amino acids, the production of 4′-OH-CB79 decreased, whereas that of the dechlorinated metabolite 4′-OH-CB35 increased. These results are explained by a shift in the CB77 positions toward the heme. This study provides insight into the development of enzymes with high metabolizing activity and clarifies the structural basis of PCB metabolism, as dechlorination contributes to a drastic decrease in dioxin-like toxicity.

KEYWORDS: cytochrome P450 monooxygenase, dechlorination, dioxin-like polychlorinated biphenyl, docking model, hydroxylation, 3,3′,4,4′-tetrachlorobiphenyl

1. Introduction

Cytochrome P450 (P450 or CYP) monooxygenases are heme proteins widely distributed in microorganisms, plants, and animals. They play an important role in the oxidative reactions involved in the biosynthesis of endogenous compounds and the xenobiotic metabolism of hydrophobic compounds. Particularly, the mammalian CYP1–3 families are involved in metabolizing xenobiotics such as pesticides and environmental pollutants (Inui et al., 2001). The substrate-binding cavity is situated in the P450 enzyme, and the heme iron, located at the cavity's bottom, activates an oxygen molecule using electrons from NADPH. The substrate-binding cavities of P450 enzymes can accommodate various chemicals with different structures and use them as substrates. Therefore, one P450 species can oxidize multiple types of xenobiotics.

Polychlorinated biphenyls (PCBs) are chemically stable and thus are widely used in commercial products such as transformers and condensers. However, because of their extremely hydrophobic and persistent chemical properties, PCBs released into the environment accumulate in apex predators through food chains. Accumulation of high levels of PCBs in animals causes adverse effects, including carcinogenicity and teratogenicity. Therefore, PCBs have been registered as persistent organic pollutants (http://www.pops.int). Although there are theoretically 209 PCB congeners, 12 PCBs with a planar structure have dioxin-like toxicity. These 12 congeners are known as dioxin-like PCBs and have toxic equivalency factor (TEF) values reflecting the extent of their toxicity (Van den Berg et al., 2006). Therefore, the metabolic fate of dioxin-like PCBs should be clarified to determine their toxicity.

An important step in PCB metabolism is oxidation by P450 species in the Phase I reaction. Dioxin-like PCBs are metabolized to hydroxylated (OH) metabolites by the CYP1A and CYP2B

subfamilies (Yamazaki et al., 2011; Mise et al., 2016). The non-*ortho*-substituted PCB, 3,3′,4,4′,5-pentachlorobiphenyl (CB126), which exhibits the highest dioxin-like toxicity among PCB congeners, is metabolized by rat CYP1A1 to OH-metabolites (Yamazaki et al., 2011). In contrast, human CYP2B6 metabolizes mono-*ortho* substituted PCB, 2,3′,4,4′,5-pentachlorobiphenyl (CB118) to OH-metabolites (Mise et al., 2016). Hydroxylation of PCBs contributes to detoxification by increasing their sensitivity to further detoxifying systems, such as conjugation in Phase II reactions (Yoshimura et al., 1987; Haraguchi et al., 1997). Dechlorinated OH-tetrachloro-metabolites of CB126 and CB118 are produced concomitantly with OH-pentachloro-metabolites, and dechlorination greatly decreases dioxin-like toxicity by increasing water solubility. Compared to human CYP1A1, rat CYP1A1 exhibited higher metabolizing activity toward CB126, suggesting that humans are more sensitive than rats to CB126 toxicity. In contrast, CB118 was metabolized to a greater extent by human CYP2B6 than by rat CYP1A1 and CYP2B1. These results indicate the difficulty in extrapolating metabolic data using experimental animals for human risk evaluation. Therefore, *in vitro* studies are needed to compare the metabolizing activities of rat and human P450 enzymes.

3,3′,4,4′-Tetrachlorobiphenyl (CB77) is relatively abundant in the environment and eventually accumulates in organisms (Nunes et al., 2011). The CB77 metabolites, 4′-OH-3,3′,4,5′-tetrachlorobiphenyl (CB79) and 5-OH-CB77, were detected in the feces of CB77-administered rats (Yoshimura et al., 1987). P450 species inducibly produced in hepatic microsomes prepared from rats administered with the typical CYP1A inducer 3-methylcholanthrene (MC) increased the levels of these CB77 metabolites (Ishida et al., 1991). This result suggests that CYP1A is responsible for CB77 metabolism in rats. Furthermore, metabolism studies using scup (White et al., 1997), channel catfish (Doi et al., 2006), chick embryos (Klasson Wehler et al., 1990), and

beluga and pilot whales (White et al., 1997) revealed other CB77 metabolites such as 2-OH-CB77 and 6-OH-CB79. These studies indicate that PCB metabolites differ depending on the species. However, information regarding CB77 metabolism by human CYP1A1 is limited.

In this study, the metabolic activities of recombinant rat and human CYP1A1s toward CB77 were measured, and their differences in CB77 metabolism were clarified by comparing their 3D structures and docking models with CB77. Rat and human CYP1A1s have a high amino acid identity (79%) and similar 3D structures (Yamazaki et al., 2011). Thus, amino acids responsible for the differences in the metabolic activities of CB77 between rat and human CYP1A1s can be identified.

2. Materials and methods

2.1. Chemicals and reagents

Microsomes from insect cells expressing rat or human *CYP1A1* and rat or human NADPH-cytochrome P450 oxidoreductase genes were purchased from BD Biosciences (San Jose, CA, USA). CB77 (AccuStandard, New Haven, CT, USA) was dissolved in dimethyl sulfoxide (DMSO) to a final concentration of 2,000 μg/mL. A ^{13}C-Labeled OH-PCB mixture, used as the internal standard, and [$^{13}C_{12}$]-2,3′,4′,5-tetrachlorobiphenyl, used as the syringe spike, were purchased from Wellington Laboratories (Ontario, Canada).

2.2. Measurement of catalytic activities of rat and human CYP1A1s and their mutants toward CB77

The reaction mixtures contained CB77 at a final DMSO concentration of 0.1% (v/v), microsomes containing 80 nM of either rat or human CYP1A1, 3.3 mM magnesium chloride, and an NADPH regeneration system (5 mM glucose-6-phosphate and 1 U of glucose-6-phosphate dehydrogenase) in 100 mM potassium phosphate buffer at pH 7.4. This mixture was allowed to react for 2 h at 37 °C following the addition of NADPH at a final concentration of 0.5 mM. After adding 10 μL of 100 ng/mL ^{13}C-labeled OH-PCB mixture as an internal standard, the metabolites were extracted with four volumes of hexane and methylated as described previously (Sakiyama et al., 2007). OH-PCBs were identified and quantified using a high-resolution gas chromatography-mass spectrometer (HRGC/HRMS) under previously described conditions (Goto et al., 2018). The catalytic activities of rat and human CYP1A1s and their mutants produced in the microsomal fractions of recombinant *Saccharomyces cerevisiae* toward CB77 were also measured.

2.3. Construction of rat and human CYP1A1 mutants

Rat and human *CYP1A1* genes in pUC18 were transferred into the *Escherichia coli* strain JM109. Site-directed mutagenesis was performed using the QuikChange Multi Site-Directed Mutagenesis Kit (Agilent Technologies, Santa Clara, CA, USA) with primers containing T946C and G358T mutations for rat *CYP1A1* and G936T, A346G, and G347C mutations for human *CYP1A1* (Table S1). These mutations were confirmed using DNA sequencing. Rat and human *CYP1A1* mutant coding sequences were inserted at the *Hin*dIII sites of the pGYR expression plasmid containing yeast NADPH–cytochrome P450 oxidoreductase (*YR*) genes, resulting in the pGYR/r1A1mutant and pGYR/h1A1mutant, respectively. Plasmids containing cDNAs of wild-type rats and human CYP1A1s were also constructed and introduced into the *S. cerevisiae* AH22 strain using a one-step yeast transformation method (Chen et al., 1992).

2.4. Preparation of microsomal fractions from recombinant S. cerevisiae

Recombinant *S. cerevisia*e AH22/pGYRr1A1, AH22/pGYRr1A1mutant, AH22/pGYRh1A1, and AH22/pGYRh1A1mutant cells expressing rat *CYP1A1*, rat *CYP1A1* mutant, human *CYP1A1*, and human *CYP1A1* mutant, respectively, as well as *YR* genes were pre-cultured in synthetic minimum medium containing 8% (w/v) glucose, 0.67% (w/v) yeast nitrogen base without amino acids, and 160 mg/L L-histidine for 20 h at 30 °C. The culture was then transferred to medium containing 8% (w/v) glucose, 1% (w/v) yeast extract, 2% (w/v) peptone, and 40 mg/L adenine sulfate and incubated for 20 h at 30 °C. Microsomal fractions were prepared as previously described (Oeda et al., 1985). Protein concentrations were measured using the Bradford method (Bradford, 1976) with bovine serum albumin as the standard. The amounts of P450s in the microsomal fractions were determined from the reduced CO difference spectra (Omura and Sato, 1964). The levels of rat and human CYP1A1s and rat and human CYP1A1 mutants in the microsomes were 110, 24.2, 15.8, and 7.61 pmol/mg microsomal protein, respectively (Table S2).

2.5. Measurement of 7-ethoxycoumalin O-*deethylation activity of CYP1A1s*

The 7-ethoxycoumalin *O*-deethylation (ECOD) activities of rat and human CYP1A1s and their mutants in the yeast microsomal fractions were measured. The reaction mixture (0.5 mL) contained 0.26 mM 7-ethoxycoumarin dissolved in 60% (v/v) methanol; microsomes containing 80 nM of either rat, human CYP1A1, or their mutants; and an NADPH regeneration system in 100 mM potassium phosphate buffer at pH 7.4. The reaction was initiated by adding NADPH at a final concentration of 0.5 mM. After incubation for 1 h at 37 °C and the addition of 30% (v/v) trichloroacetic acid, the reactants were vortexed and centrifuged at 2,000 rpm for 5 min at 4 °C. The supernatant (400 μL) was separated and mixed with a 2-fold volume of chloroform. The

organic phase (500 μL) was collected and mixed with 1 mL of 0.01 M sodium hydroxide and 0.1 M sodium chloride. After centrifugation at 12,000 rpm for 5 min at 4 °C, the supernatant was collected, and fluorescence was measured at excitation and emission wavelengths of 366 and 452 nm, respectively.

2.6. Homology modeling and substrate docking

In previous studies, a 3D model of human CYP1A1 was constructed based on the X-ray crystal structure of human CYP1A2 (Sansen et al., 2007; Itoh et al., 2010), and then a 3D model of rat CYP1A1 based on the human CYP1A1 model was constructed (Yamazaki et al., 2011). Models of the rat and human CYP1A1 mutants based on the rat and human CYP1A1 models, respectively, were constructed using the "Mutate monomers" tool in SYBYL Biopolymer (Tripos, St Louis, MO, USA).

Docking was performed using Surflex Dock in SYBYL 8.0 (Tripos), as previously described (Yamazaki et al., 2011). Human and rat CYP1A1 models and their mutants were used as the CYP protein structure. Diverse substrate structure orientations for rat and human CYP1A1s, their mutants, and selected substrate structures with the top 25 ranked candidates based on the weighted sum of the scoring functions were obtained.

3. Results and discussion

3.1. Catalytic activity of rat and human CYP1A1s toward CB77

Chromatographic peaks corresponding to methylated mono-OH tetrachlorobiphenyl M1 and methylated mono-OH trichlorobiphenyl M2 increased in intensity when microsomes containing

rat CYP1A1s in the presence of NAPDH were analyzed (Fig. 1C–F). In contrast, only M1 was detected in an NADPH-dependent manner when microsomes containing human CYP1A1 were used (Fig. 1G–J). Control microsomes that did not contain any CYP1A1 showed no peaks (Fig. S1). The pattern of retention times of M1 and M2 were identical to those of the authentic standard S1, which is 5-MeO-2,3′,4,4′-tetrachlorobiphenyl (CB66) or 4′-MeO-CB79, and S2, which is 4′-MeO-3,3′,4-trichlorobiphenyl (CB35) (Fig. 1A–D, G, H). These M1 and M2 peaks also matched the isotope ratios ($[M]^+$:$[M+2]^+$) of the authentic standards S1 and S2, indicating that the peaks were from tetra- and trichlorinated compounds, respectively (Fig. S2). In addition, the patterns of fragment ions in the mass spectrum were examined to determine the position of the OH-group on the biphenyl ring (Fig. S3). The upper $[M\text{-}CH_3Cl]^+$ and lower $[M\text{-}COCH_3]^+$ peaks indicated that the substituted OH-group was at the *ortho*- and *meta*- or *para*-positions, respectively (Kunisue and Tanabe, 2009). The M1 peak was observed in both $[M\text{-}CH_3Cl]^+$ and $[M\text{-}COCH_3]^+$ with the same intensity, indicating that M1 could have an OH-group in all positions, and the M2 peak was observed in $[M\text{-}COCH_3]^+$, indicating that M2 had an OH-group in the *meta*- or *para*-position. A comparison of the retention times of the authentic standards and isotope ratios indicated that M1 was 5-OH-CB66 or 4′-OH-CB79. Considering previous studies of CB77 metabolism (Ishida et al., 1991; Murk et al., 1994; Morse et al., 1995), we predicted that M1 is 4′-OH-CB79, produced by hydroxylation of the 4-position in the biphenyl ring through the epoxide intermediate followed by migration of a chlorine atom caused by an NIH shift from the 4- to the 5-position (Gordon et al., 1967). This prediction is reasonable because it is unlikely that 5-OH-CB66 is produced by hydroxylation at the 5-position followed by migration of a chlorine atom from the 3- to 2-position. In contrast, M2 was identified as 4′-OH-CB35 by hydroxylation and dechlorination of the 4-position through electrophilic substitution (Hackett et al., 2007).

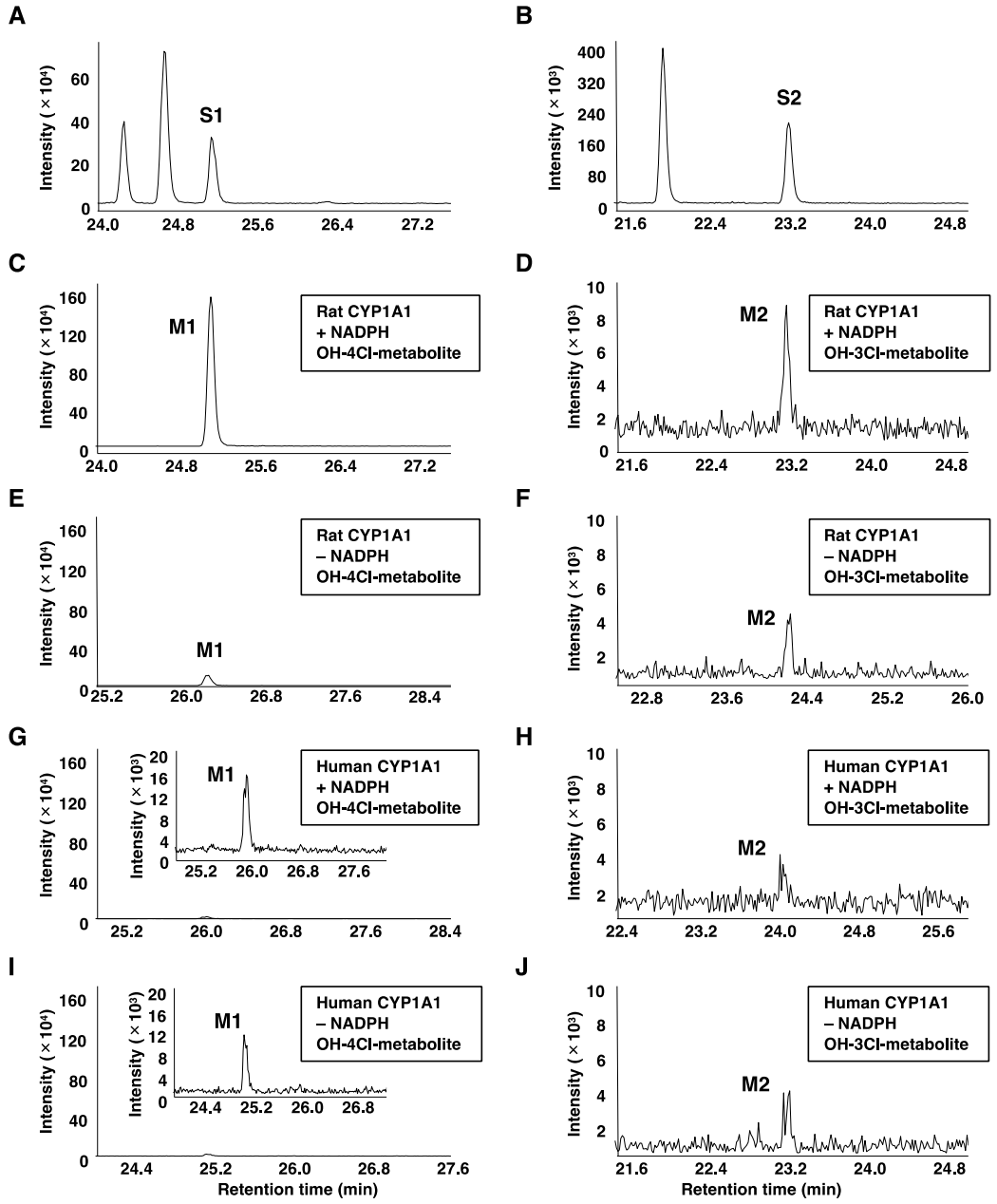

198

199 **Fig. 1.** Detection of tetrachlorobiphenyl (C, E, G, I) and trichlorobiphenyl (D, F, H, J) metabolites
200 from 3,3′,4,4′-tetrachlorobiphenyl (CB77) reacted with rat (C–F) and human (G–J) CYP1A1s by
201 high-resolution gas chromatography/high-resolution mass spectrometry. A and B, peak S1, 5-
202 MeO-2,3′,4,4′- or 4′-MeO-3,3′,4,5′-tetrachlorobiphenyl; peak S2, 4′-MeO-3,3′,4-trichlorobiphenyl.
203 C and D, rat CYP1A1 with NADPH. E and F, rat CYP1A1 without NADPH. G and H, human

CYP1A1 with NADPH. I and J, human CYP1A1 without NADPH. The insets in G and I show the magnified graphs.

Both peaks corresponding to M1 and M2 in the microsomes containing rat CYP1A1 were much larger than those containing human CYP1A1. The kinetic parameters of rat and human CYP1A1s for the production of 4′-OH-CB79 and 4′-OH-CB35 were determined using the Michaelis–Menten equation (Fig. S4A–C) and Lineweaver–Burk plot (Fig. S4D–F). The V_{max}/K_m of rat CYP1A1 toward the production of 4′-OH-CB79 was >150-fold higher than that of human CYP1A1 (Table 1). Similarly, the V_{max}/K_m of rat CYP1A1 toward the production of 4′-OH-CB35 was 2.68, whereas 4′-OH-CB35 was not detected in human CYP1A1. These results indicate that rat CYP1A1 has much higher activity toward CB77 metabolism than human CYP1A1. Fig. 2 shows the proposed metabolic pathways for CB77 based on rat and human CYP1A1s. The OH-metabolites generated by the NIH shift and dechlorination were also detected in previous studies (Liu et al., 2020). The feces from intraperitoneally CB77-injected rats contained 5-OH-CB77 and 4′-OH-CB79 as major metabolites and 4′-OH-CB35 as a minor metabolite (Yoshimura et al., 1987; Koga et al., 1989). The livers of rats orally administered with CB77 contained a higher level of 4′-OH-CB79 compared to the level of 5-OH-CB77 (Morse et al., 1995). In *in vitro* experiments using liver microsomes from rats treated with MC, 4′-OH-CB79 was detected as a major metabolite (Ishida et al., 1991). Another *in vitro* experiment using the CYP1A inducer β-naphthoflavone revealed the production of 4′-OH-CB79, 5-OH-CB77, and 6-OH-CB77 (Morse et al., 1995). These results strongly suggest that CYP1A1 is responsible for CB77 metabolism and that 4′-OH-CB79 is a primary metabolite.

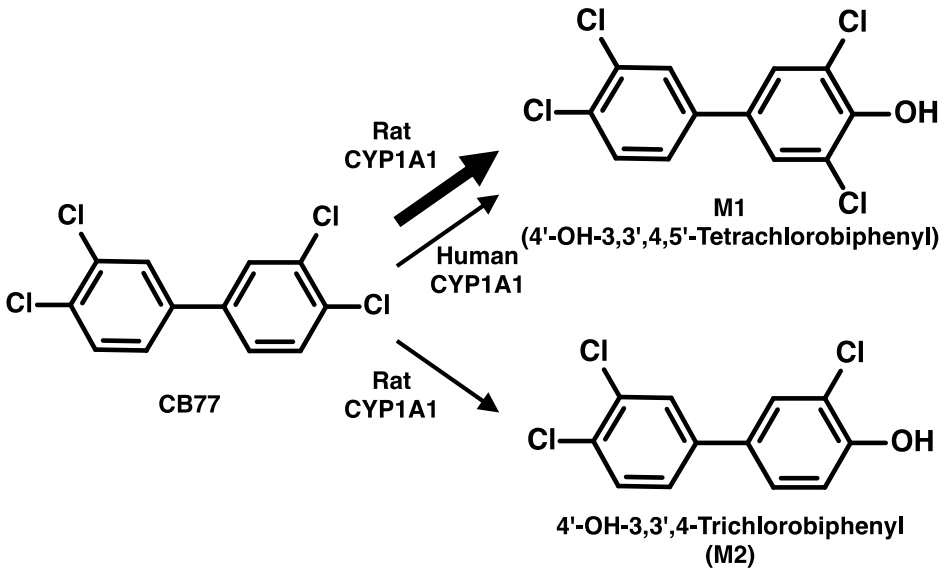

225

226 **Fig. 2.** Proposed metabolic pathways of 3,3′,4,4′-tetrachlorobiphenyl (CB77) by rat and human
227 CYP1A1s. M1 was predicted as 4′-OH-3,3′,4,5′-tetrachlorobiphenyl and M2 was identified as 4′-
228 OH-3,3′,4-trichlorobiphenyl.

229

230 *3.2. Docking studies of rat and human CYP1A1s with CB77*

231 The substrate-binding cavities of rat and human CYP1A1s were well-conserved except for four
232 residues in rat (A120, T126, S225, and F316) and human (S116, S122, N221, and L312) CYP1A1s
233 (Yamazaki et al., 2011). Two of the four residues (A120 and F316 in rat CYP1A1; S116 and L312
234 in human CYP1A1) caused a large spatial structural change, resulting in a difference in the cavity
235 volumes (510 $Å^3$ in rat CYP1A1 and 600 $Å^3$ in human CYP1A1). For CB126 metabolism, the
236 smaller volume of the rat CYP1A1 cavity resulted in a more stable accommodation of CB126
237 when compared with the human CYP1A1, resulting in the high metabolizing activity of rat
238 CYP1A1 (Yamazaki et al., 2011).

239 Docking studies of rat and human CYP1A1s with CB77 were performed to understand their
240 interaction. CB77 showed distinct orientations in each CYP1A1; the structures were classified into
241 three and six orientations toward rat and human CYP1A1s, respectively (Fig. 3A, B). As rat
242 CYP1A1 accommodates CB77 with fewer orientations than human CYP1A1, CB77 is stable in
243 the substrate-binding cavity of rat CYP1A1, leading to high activity. Furthermore, all orientations
244 in rat CYP1A1 were directed to the iron atom of heme, which is the active center of P450s. In
245 contrast, human CYP1A1 accommodates CB77 in multiple orientations, and most of the
246 orientations of CB77 in human CYP1A1 are distant from the heme iron. CB77 was less than 5 Å
247 from the heme iron in eight and three conformations in rat and human CYP1A1, respectively (Fig.
248 3C, D). Proximity is an important factor related to the high activity (Yamazaki et al., 2011), and a
249 distance of 5 Å is sufficient for CB77 to react with CYP1A1s. These results indicate that rat
250 CYP1A1 shows higher activity than human CYP1A1 because of the stable accommodation and
251 proximity of CB77. Docking studies also provided insight into the hydroxylation position of CB77.
252 The 4-position of CB77 accessed the heme, supporting that 4′-OH-CB79 and 4′-OH-CB35 were
253 produced.

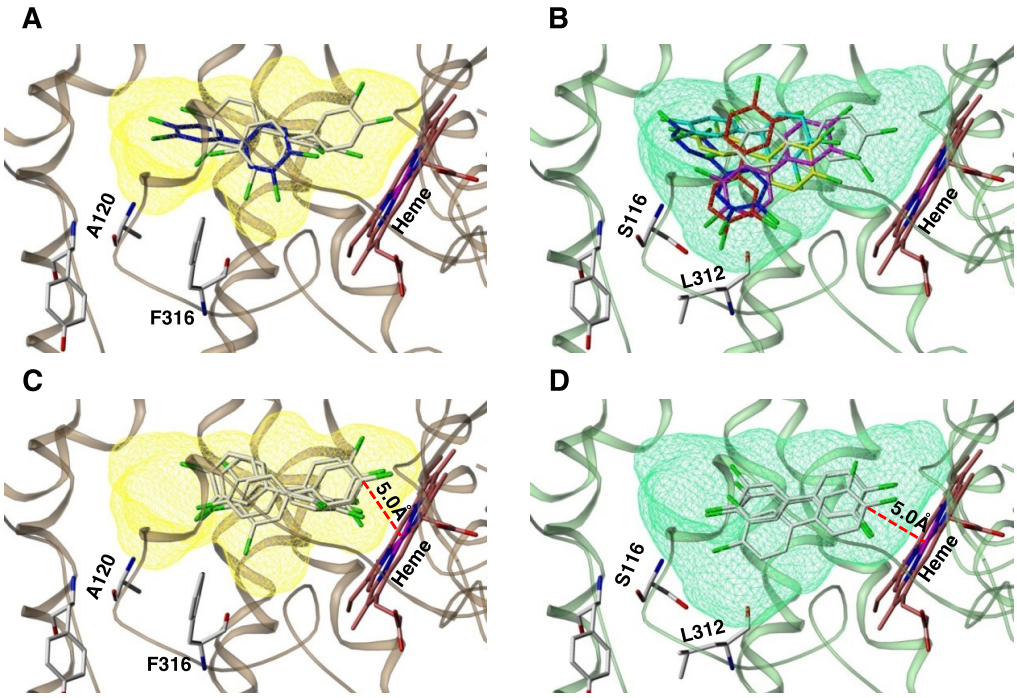

Fig. 3. Docking models of rat (A, C) and human (B, D) CYP1A1s with 3,3′,4,4′-tetrachlorobiphenyl (CB77). The Connolly channel surfaces of the cavities are displayed using a colored mesh. A and B depict representative orientations of CB77 in the substrate-binding cavity of rat (three orientations) and human (six orientations) CYP1A1s; C and D depict the conformations of CB77 close to the heme iron (less than 5 Å) in rats (eight conformations) and human (three conformations) CYP1A1s.

The dechlorinated OH-metabolite M2 was detected at much lower levels than the OH-metabolite M1 (Fig. 1C, D). CB77 has a TEF value of 0.0001, indicating that dioxin-like toxicity is caused by CB77 accumulation in mammals (Van den Berg et al., 2006). However, no trichlorinated biphenyls showed a TEF value, suggesting that dechlorination of

266 tetrachlorobiphenyls eliminates dioxin-like toxicity. Thus, the mechanisms underlying the
267 dechlorination of CB77 were evaluated using docking models.

268 CB77 shows two conformations (conformations A and B, Fig. 4) in the substrate-binding cavity
269 of rat CYP1A1 close to the heme. The 4- and 5- and the 3- and 4-positions of CB77 are directed
270 to the oxygen atom of heme in conformations A and B, respectively. Because both the 4- and 5-
271 positions of CB77 are equally close to the oxygen atom in conformation A, 4,5-epoxide is formed,
272 resulting in an NIH shift of the chlorine group from the 4- to the 5-position. This reaction results
273 in the formation of 4′-OH-CB79 (metabolite M1) and not 5′-OH-CB77. In contrast, the 3- and 4-
274 positions of CB77 are sufficiently close (<4 Å) to the oxygen atom to form epoxide (Fig. 4) (Hata
275 et al., 2008). However, if epoxidation occurs, the final product cannot be a phenolic compound.
276 Therefore, electrophilic substitution should be performed to form dechlorinated OH-metabolite
277 M2. An electrophilic attack occurs at the 4-position of CB77 by the oxygen atom, resulting in the
278 elimination of the chlorine atom (Hackett et al., 2007). However, it is difficult to show the
279 advantages of conformation A, although more M1 than M2 is produced. To this end, there are two
280 possibilities: first, steric hindrance between the chlorine group at the 3-position in conformation B
281 and Thr126, which comprise the substrate-binding cavity; and second, the efficiency of
282 epoxidation, which is much higher than that of electrophilic substitution.

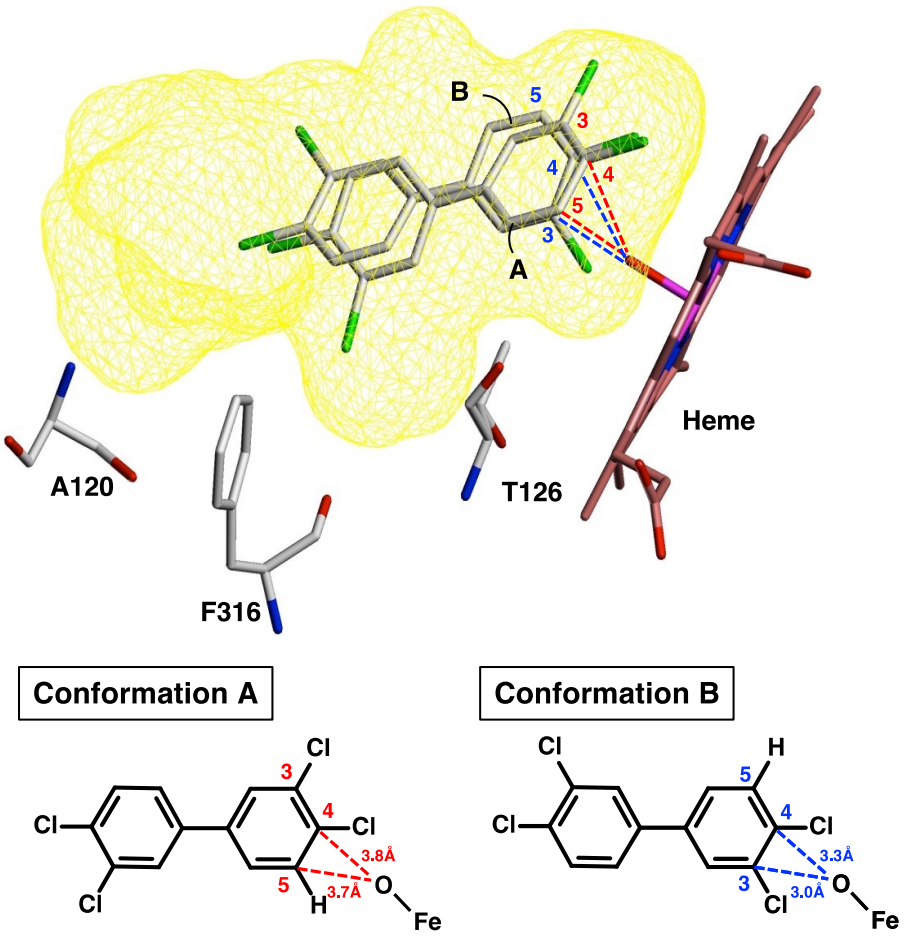

283

284 **Fig. 4.** Proposed conformations of 3,3′,4,4′-tetrachlorobiphenyl (CB77) in the substrate-binding
285 cavity of rat CYP1A1 to produce hydroxylated tetrachlorobiphenyl and hydroxylated
286 trichlorobiphenyl metabolites. Conformations A and B of CB77 produced M1, predicted as 4′-OH-
287 3,3′,4,5′-tetrachlorobiphenyl, and M2, identified as 4′-OH-3,3′,4-trichlorobiphenyl.

288

289 *3.3. Measurement of metabolic activities of CYP1A1 mutants*

290 Two amino acids constituting the substrate-binding cavity of rat and human CYP1A1s play
291 important roles in CB126 metabolism (Yamazaki et al., 2011). Therefore, the reciprocal mutations
292 A120S and F319L were introduced in rat CYP1A1, and S116A and L312F were introduced in

293 human CYP1A1 to clarify the importance of these amino acids in CB77 metabolism. The mutated
294 sites of *CYP1A1* genes were confirmed using DNA sequencing (Fig. S5). After introducing
295 plasmids containing each *P450* into *S. cerevisiae*, the P450 content was determined from the
296 reduced CO difference spectra in the microsomes. All microsomes showed absorption maxima at
297 approximately 450 nm, but their contents varied among the P450s (Fig. S6 and Table S2). The
298 P450 content of each mutant was lower than that of the wild-type, and the production of rat
299 CYP1A1 was higher than that of human CYP1A1. Human CYP1A1 and its mutant were not stably
300 produced in *S. cerevisiae* compared with rat CYP1A1 and its mutant.

301 The ECOD activity of the microsomes containing rat CYP1A1 mutant decreased significantly
302 by 10% compared with that of wild-type rat CYP1A1 (Table S2). In contrast, mutant human
303 CYP1A1 showed significantly higher activity (2.4-fold) than wild-type human CYP1A1.
304 Therefore, the two amino acids may be responsible for metabolic activity by changing the shape
305 and volume of the substrate-binding cavity.

306 Rat CYP1A1 mutant showed a decrease in hydroxylation activity to produce M1 at all tested
307 concentrations of CB77 (Fig. S7A). The V_{max}/K_m in the mutant enzyme decreased by
308 approximately 30% compared to that in the wild-type enzyme (Table 2). In contrast, the mutant
309 enzyme showed higher production of M2, which is a dechlorinated OH-metabolite, compared to
310 that of the wild-type enzyme (Fig. S7B). The activity of the mutant enzyme was 3.9-fold higher
311 than that of the wild-type enzyme (Table 2). This result was unexpected because mutation of amino
312 acids in rat CYP1A1 to a human CYP1A1 led to decreased ECOD activity and production of M1.
313 In contrast, human CYP1A1 and its mutant showed no hydroxylation activity, possibly because
314 two other amino acids, T126 and S225, which comprise the substrate-binding cavity of rat
315 CYP1A1, are also important for CB77 metabolism.

316 *3.4. Docking studies of rat and human CYP1A1 mutants with CB77*

317 CB77 in the substrate-binding cavity of rat and human CYP1A1 mutants showed five and four
318 orientations, respectively (Fig. S8A, B). With these mutations, the cavity of rat CYP1A1 mutant
319 was enlarged, and orientations not directed to the heme emerged (Fig. S8A). Concomitantly, the
320 conformations of CB77 in the cavity were scattered (Fig. S8C), resulting in unstable
321 accommodation of CB77 in the cavity and low metabolizing activities. In contrast, the cavity shape
322 of the human CYP1A1 mutant was similar to that of the rat CYP1A1 wild-type after the
323 introduction of F312, and most orientations were directed to the heme (Fig. 3A and Fig. S8B). As
324 a result, the number of conformations close to the heme increased (Fig. S8D). As human CYP1A1
325 mutant with mutations at S116A and L312F did not metabolize CB77, the mutant containing
326 S122T and N221S will be used in further studies.

327 The detailed mechanisms of the contrasting activities toward M1 and M2 production were
328 examined in docking studies. In wild-type rat CYP1A1, the phenyl ring of F316 squeezes the 4-
329 and 5-positions of CB77 close to the heme at distances of 4.9 and 4.8 Å, respectively, resulting in
330 the production of M1 (Fig. S9A, CB77 shown in red). In contrast, the rat CYP1A1 mutant F316L
331 without a phenyl ring cannot squeeze CB77, leading to a distance of 5.4 Å between the 5-position
332 and heme (Fig. S9A, CB77 shown in blue), thereby conferring low hydroxylation activity towards
333 CB77 with an NIH shift. Dechlorinated OH-metabolite M2 showed higher production in the
334 mutant than in the wild-type; the bulky side-chain of F316 limits the conformation of CB77
335 because of the vicinity (2.4 Å) of the chlorine group at the 3′-position of CB77 (Fig. S9B). In
336 contrast, after introducing F316L, conformations without conflicts and whose 3- and 4-positions
337 were close to the heme tended to increase, as described in two conformations of CB77 in blue

compared with one conformation in red. These effects led to an increase in the dechlorination activity of the mutant.

4. Conclusions

We predicted the structural basis of CB77 metabolism by rat and human CYP1A1s. We concluded that stable accommodation of CB77 in the substrate-binding cavity and the proximity of CB77 to heme are important for achieving efficient hydroxylation and dechlorination. Rat CYP1A1 showed much higher hydroxylation and dechlorination activities compared with human CYP1A1. These results are consistent with the metabolism of CB126 (Yamazaki et al., 2011) and suggest that humans have low metabolizing activities toward dioxin-like PCBs compared with rat CYP1A1. These PCBs have high TEF values among PCB congeners, indicating that they cause dioxin-like toxicity in human bodies. This suggests that humans are more sensitive to dioxin-like PCBs than experimental animals, such as rats. The underlying mechanisms were determined by identifying the amino acids responsible for CB77 metabolism. Detailed dechlorination mechanisms were proposed by constructing docking models; however, enhanced metabolic activity toward CB77 by the human CYP1A1 mutant was not observed. Further studies are needed to evaluate whether other amino acid mutations in the substrate-binding cavity of human CYP1A1 can affect CB77 metabolism. Determining the dechlorination mechanisms will lead to the development of metabolizing enzymes that can drastically decrease dioxin-like toxicity (Yoshimura et al., 1987). A promising approach to utilizing such enzymes is phytoremediation. Several P450 species have been introduced into transgenic plants to degrade PCBs (Aken et al.,

2010; Shimazu et al., 2011). Dechlorination-enhanced mutants are a prospective tool for cleaning dioxin-like PCBs in contaminated environments.

Author Contributions

Miku Yabu: Data curation, Formal analysis, Investigation, Roles/Writing - original draft. **Yuki Haga** : Data curation, Formal analysis, Investigation. **Toshimasa Itoh** : Data curation, Formal analysis, Investigation. **Erika Goto**: Data curation, Investigation. **Motoharu Suzuki** : Data curation, Formal analysis, Investigation. **Kiyoshi Yamazaki** : Data curation, Formal analysis, Investigation. **Shintaro Mise** : Data curation, Investigation. **Keiko Yamamoto**: Data curation, Formal analysis, Validation. **Chisato Matsumura** : Data curation, Validation. **Takeshi Nakano**: Methodology, Validation. **Toshiyuki Sakaki**: Methodology, Validation. **Hideyuki Inui**: Conceptualization, Data curation, Funding acquisition, Project administration, Roles/Writing - original draft.

Funding Sources

This work was supported by the Ministry of Agriculture, Forestry and Fisheries of Japan [grant number HC-06-2311-1 to HI] and Genomics for Agricultural Innovation [grant number GMB-0006 to HI].

Acknowledgments

We thank Yuko Ishida and Harunobu Tsuzuki for sample preparation. We would like to thank Editage (www.editage.com) for English language editing.

Table 1 Kinetic parameters of rat and human CYP1A1s for hydroxylation and dechlorination of 3,3′,4,4′-tetrachlorobiphenyl (CB77).

CYP1A1	4′-OH-3,3′,4,5′-Tetrachlorobiphenyl			4′-OH-3,3′,4-Trichlorobiphenyl		
	K_m [1]	V_{max} [2]	V_{max}/K_m	K_m	V_{max}	V_{max}/K_m
Rat	10.3	1590	153	3.60	9.66	2.68
Human	7.74	7.54	0.975	ND[3]	ND	-

[1] μM; [2] pmol/min/(nmol P450); [3] not detected.

Table 2 Kinetic parameters of rat CYP1A1 and its mutant for hydroxylation and dechlorination of 3,3′,4,4′-tetrachlorobiphenyl (CB77).

Rat CYP1A1	4′-OH-3,3′,4,5′-Tetrachlorobiphenyl			4′-OH-3,3′,4-Trichlorobiphenyl		
	K_m [1]	V_{max} [2]	V_{max}/K_m	K_m	V_{max}	V_{max}/K_m
WT	7.47	830	111	53.4	238	4.46
Mutant	4.99	375	75.2	2.18	38.5	17.6

[1] μM; [2] pmol/min/(nmol P450)

References

Van Aken, B., Correa, P.A., Schnoor, J.L., 2010. Phytoremediation of polychlorinated biphenyls: new trends and promises. Environ. Sci. Technol. 44, 2767–2776. https://doi.org/10.1021/es902514d.

Bradford, M.M., 1976. A rapid and sensitive method for the quantitation of microgram quantities of protein utilizing the principle of protein-dye binding. Anal. Biochem. 72, 248–254. https://doi.org/10.1016/0003-2697(76)90527-3.

Chen, D.C., Yang, B.C., Kuo, T.T., 1992. One-step transformation of yeast in stationary phase. Curr. Genet. 21, 83–84. https://doi.org/10.1007/BF00318659.

Doi, A.M., Lou, Z., Holmes, E., Venugopal, C.S., Nyagode, B., James, M.O., Kleinow, K.M., 2006. Intestinal bioavailability and biotransformation of 3,3′,4,4′- tetrachlorobiphenyl (CB 77) in in situ preparations of channel catfish following dietary induction of CYP1A. Aquat. Toxicol. 77, 33–42. https://doi.org/10.1016/j.aquatox.2005.10.013.

Gordon, G., Daly, J.W., Jerina, D.M., Renson, J., Witkop, B., Udenfriend, S., 1967. Hydroxylation-induced migration: The NIH shift. Science 157, 1524–1530. https://doi.org/10.1126/science.157.3796.1524.

Goto, E., Haga, Y., Kubo, M., Itoh, T., Kasai, C., Shoji, O., Yamamoto, K., Matsumura, C., Nakano, T., Inui, H., 2018. Metabolic enhancement of 2,3′,4,4′,5-pentachlorobiphenyl (CB118) using cytochrome P450 monooxygenase isolated from soil bacterium under the presence of perfluorocarboxylic acids (PFCAs) and the structural basis of its metabolism. Chemosphere 210, 376–383. https://doi.org/10.1016/j.chemosphere.2018.07.026.

412 Hackett, J.C., Sanan, T.T., Hadad, C.M., 2007. Oxidative dehalogenation of perhalogenated
413 benzenes by cytochrome P450 compound I. Biochemistry 46, 5924–5940.
414 https://doi.org/10.1021/bi700365x.

415 Haraguchi, K., Kato, Y., Masuda, Y., Kimura, R., 1997. Metabolism of 3,3′,4,4′-
416 tetrachlorobiphenyl via sulphur-containing pathway in rat: liver-specific retention of
417 methylsulphonyl metabolite. Xenobiotica. 27, 831–842.
418 https://doi.org/10.1080/004982597240190.

419 Hata, M., Tanaka, Y., Kyoda, N., Osakabe, T., Yuki, H., Ishii, I., Kitada, M., Neya, S., Hoshino,
420 T., 2008. An epoxidation mechanism of carbamazepine by CYP3A4. Bioorganic Med. Chem.
421 16, 5134–5148. https://doi.org/10.1016/j.bmc.2008.03.023.

422 Inui, H., Shiota, N., Motoi, Y., Ido, Y., Inoue, T., Kodama, T., Ohkawa, Y., Ohkawa, H., 2001.
423 Metabolism of herbicides and other chemicals in human cytochrome P450 species and in
424 transgenic potato plants co-expressing human CYP1A1, CYP2B6 and CYP2C19. J. Pestic.
425 Sci. 26, 28–40. https://doi.org/10.1584/jpestics.26.28.

426 Ishida, C., Koga, N., Hanioka, N., Saeki, H.K., Yoshimura, H., 1991. Metabolism *in vitro* of
427 3,4,3′,4′- and 2,5,2′,5′-tetrachlorobiphenyl by rat liver microsomes and highly purified
428 cytochrome P-450. J. Pharmacobiodyn. 14, 276–284.
429 https://doi.org/10.1248/bpb1978.14.276.

430 Itoh, T., Takemura, H., Shimoi, K., Yamamoto, K., 2010. A 3D model of CYP1B1 explains the
431 dominant 4-hydroxylation of estradiol. J. Chem. Inf. Model. 50, 1173–1178.
432 https://doi.org/10.1021/ci1000554.

433 Klasson Wehler, E., Brunström, B., Rannug, U., Bergman, Å., 1990. 3,3′,4,4′-
434 Tetrachlorobiphenyl: Metabolism by the chick embryo in ovo and toxicity of hydroxylated
435 metabolites. Chem. Biol. Interact. 73, 121–132. https://doi.org/10.1016/0009-
436 2797(90)90112-Z.

437 Koga, N., Beppu, M., Ishida, C., Yoshimura, H., 1989. Further studies on metabolism in vivo of
438 3,4,3′,4′-tetrachlorobiphenyl in rats: Identification of minor metabolites in rat faeces.
439 Xenobiotica 19, 1307–1318. https://doi.org/10.3109/00498258909043182.

440 Kunisue, T., Tanabe, S., 2009. Hydroxylated polychlorinated biphenyls (OH-PCBs) in the blood
441 of mammals and birds from Japan: Lower chlorinated OH-PCBs and profiles. Chemosphere
442 74, 950–961. https://doi.org/10.1016/j.chemosphere.2008.10.038.

443 Liu, J., Tan, Y., Song, E., Song, Y., 2020. A critical review of polychlorinated biphenyls
444 metabolism, metabolites, and their correlation with oxidative stress. Chem. Res. Toxicol. 33,
445 2022–2042. https://doi.org/10.1021/acs.chemrestox.0c00078.

446 Mise, S., Haga, Y., Itoh, T., Kato, A., Fukuda, I., Goto, E., Yamamoto, K., Yabu, M., Matsumura,
447 C., Nakano, T., Sakaki, T., Inui, H., 2016. Structural determinants of the position of
448 2,3′,4,4′,5-pentachlorobiphenyl (CB118) hydroxylation by mammalian cytochrome P450
449 monooxygenases. Toxicol. Sci. 152, 340–348. https://doi.org/10.1093/toxsci/kfw086.

450 Morse, D.C., Van Bladeren, P.J., Klasson Wehler, E., Brouwer, A., 1995. β-Naphthoflavone- and
451 self-induced metabolism of 3,3′,4,4′-tetrachlorobiphenyl in hepatic microsomes of the male,
452 pregnant female and foetal rat. Xenobiotica 25, 245–260.
453 https://doi.org/10.3109/00498259509061849.

454 Morse, D.C., Klasson Wehler, E., van de Pass, M., de Bie, A.T.H.J., Bladeren, P.J. Van, Brouwer,
455 A., 1995. Metabolism and biochemical effects of 3,3′,4,4′-tetrachlorobiphenyl in pregnant
456 and fetal rats 95, 41–56. https://doi.org/10.1016/0009-2797(94)03347-1

457 Murk, A., Morse, D., Boon, J., Brouwer, A., 1994. In vitro metabolism of 3,3′,4,4′-
458 tetrachlorobiphenyl in relation to ethoxyresorufin-*O*-deethylase activity in liver microsomes
459 of some wildlife species and rat. Eur. J. Pharmacol. Environ. Toxicol. 270, 253–261.
460 https://doi.org/10.1016/0926-6917(94)90069-8.

461 Nunes, M., Marchand, P., Vernisseau, A., Bizec, B. Le, Ramos, F., Pardal, M.A., 2011. PCDD/Fs
462 and dioxin-like PCBs in sediment and biota from the Mondego estuary (Portugal).
463 Chemosphere 83, 1345–1352. https://doi.org/10.1016/j.chemosphere.2011.02.081.

464 Oeda, K., Sakaki, T., Ohkawa, H., 1985. Expression of rat liver cytochrome P-450MC cDNA in
465 Saccharomyces cerevisiae. DNA 4, 203–210. https://doi.org/10.1089/dna.1985.4.203.

466 Omura, T., Sato, R., 1964. The carbon monoxide-binding pigment of liver microsomes: I.
467 Evidence for its hemoprotein nature. J. Biol. Chem. 239, 2370–2378.
468 https://doi.org/10.1016/S0021-9258(20)82244-3.

469 Sakiyama, T., Yamamoto, A., Kakutani, N., Fukuyama, J., Okumura, T., 2007. Hydroxylated
470 polychlorinated biphenyls (OH-PCBs) in the aquatic environment: Levels and congener
471 profiles in sediments from Osaka. Japan. Organohal. Comp. 69, 1380–1383.

472 Sansen, S., Yano, J.K., Reynald, R.L., Schoch, G.A., Griffin, K.J., Stout, C.D., Johnson, E.F., 2007.
473 Adaptations for the oxidation of polycyclic aromatic hydrocarbons exhibited by the structure

of human P450 1A2. J. Biol. Chem. 282, 14348–14355. https://doi.org/10.1074/jbc.M611692200.

Shimazu, S., Inui, H., Ohkawa, H., 2011. Phytomonitoring and phytoremediation of agrochemicals and related compounds based on recombinant cytochrome P450s and aryl hydrocarbon receptors (AhRs). J. Agric. Food Chem. 59, 2870–2875. https://doi.org/10.1021/jf102561d.

Van den Berg, M., Birnbaum, L.S., Denison, M., De Vito, M., Farland, W., Feeley, M., Fiedler, H., Hakansson, H., Hanberg, A., Haws, L., Rose, M., Safe, S., Schrenk, D., Tohyama, C., Tritscher, A., Tuomisto, J., Tysklind, M., Walker, N., Peterson, R.E., 2006. The 2005 World Health Organization reevaluation of human and mammalian toxic equivalency factors for dioxins and dioxin-like compounds. Toxicol. Sci. 93, 223–241. https://doi.org/10.1093/toxsci/kfl055.

White, R.D., Shea, D., Stegeman, J.J., 1997. Metabolism of the aryl hydrocarbon receptor agonist 3,3′,4,4′-tetrachlorobiphenyl by the marine fish scup (*Stenotomus chrysops*) *in vivo* and *in vitro*. Drug Metab. Dispos. 25, 564–572.

Yamazaki, K., Suzuki, M., Itoh, T., Yamamoto, K., Kanemitsu, M., Matsumura, C., Nakano, T., Sakaki, T., Fukami, Y., Imaishi, H., Inui, H., 2011. Structural basis of species differences between human and experimental animal CYP1A1s in metabolism of 3,3′,4,4′,5-pentachlorobiphenyl. J. Biochem. 149, 487–494. https://doi.org/10.1093/jb/mvr009.

Yoshimura, H., Yonemoto, Y., Yamada, H., Koga, N., Oguri, K., Saeki, S., 1987. Metabolism i*n vivo* of 3,4,3′,4′-tetrachlorobiphenyl and toxicological assessment of the metabolites in rats. Xenobiotica 17, 897–910. https://doi.org/10.3109/00498258709044189.